Maize brace root biomechanics are determined by geometry within a genotype and material properties between genotypes

Authors: Lindsay Erndwein[1], Elahe Ganji[2,3], Ashley N. Hostetler[1], Adam Stager[1], Megan L. Killian[2,3], Erin E. Sparks[1]*

Affiliations:

[1]Department of Plant and Soil Sciences and the Delaware Biotechnology Institute, University of Delaware, Newark, DE

[2]Department of Mechanical Engineering, University of Delaware, Newark, DE

[3]Department of Orthopaedic Surgery, University of Michigan, Ann Arbor, MI

*Corresponding Author: esparks@udel.edu

Author email addresses: erndwein@udel.edu, elaganji@udel.edu, astager@udel.edu, ahende@udel.edu, mlkillia@umich.edu

Date of Submission: December 24, 2020

Number of Tables & Figures: 8 Figures

Word Count: 2,346

Number of Supplementary Tables & Figures: 3 Tables & 5 Figures

Running Title: Brace Root Biomechanics

HIGHLIGHT

Brace root biomechanics vary within and between genotypes. These results support the importance of biomechanics to define the contribution of brace roots to mechanical stability.

ABSTRACT

Crop plants are susceptible to yield loss by mechanical failure, which is called lodging. In maize (*Zea mays*), aerial nodal brace roots impart mechanical stability to plants, with previous studies showing that the lowest whorl of brace roots contributes the most. The features of brace roots that determine their contribution to mechanical stability are poorly defined. Here we tested the hypothesis that brace root mechanical properties vary between whorls, which may influence their contribution to mechanical stability. 3-point bending tests were used to determine that brace roots from the lowest whorl have the highest structural mechanical properties regardless of growth stage, and that these differences are largely due to brace root geometry within a genotype. Analysis of the brace root bending modulus determined that differences between genotypes are attributable to both geometry and material properties. These results support the role of brace root biomechanics to determine the brace root contribution to mechanical stability.

KEYWORDS

3-point bending
Anchorage
Biomechanics
Brace roots
Lodging
Maize
Nodal roots

ABBREVIATIONS

Bending Modulus (E)
Bottom Whorl (BWR)
Break Load (BL)
Computed Tomography (CT)
Digital Caliper (DC)
Middle Whorl (MWR)
Moment of Inertia (MOI)
Structural Stiffness (K)
Top Whorl (TWR)
Ultimate Load (UL)

INTRODUCTION

The increasing frequency and severity of storm systems has challenged our ability to produce crops and meet the demands of a growing world population. One outcome of severe storm systems is root and/or stem mechanical failure, which is called lodging (Berry *et al.*, 2004; Rajkumara, 2008; Fedenko *et al.*, 2015; Hostetler *et al.*, 2020). In maize (*Zea mays*), lodging causes up to 25% yield losses, with the impact of root lodging increasing as plants reach reproductive maturity (Carter and Hudelson, 1988; Flint-Garcia *et al.*, 2003; Tirado *et al.*, 2020). Plant susceptibility to lodging is influenced by plant mechanical and architectural properties, which have been well documented in stems but poorly defined in roots (Forell *et al.*, 2015; Stubbs *et al.*, 2020; Sekhon *et al.*, 2020).

The mature maize root system is predominantly composed of nodal roots, which initiate from stem nodes below (crown roots) and above (brace roots) the soil (Hoppe *et al.*, 1986; Feldman, 1994; Hochholdinger *et al.*, 2004; Hochholdinger, 2009; Blizard and Sparks, 2020). A set of brace roots emerging from a node is called whorl, and the number of brace root whorls that enter the soil positively influences lodging-resistance (Liu *et al.*, 2012; Sharma and Carena, 2016; Shi *et al.*, 2019; Reneau *et al.*, 2020). The brace root whorl closest to the soil contributes the most to stalk anchorage, with higher whorls contributing progressively less (Reneau *et al.*, 2020). However, the properties of brace roots that contribute to this variation in anchorage remain unknown.

Brace root properties that could impact anchorage include the mechanical properties of the roots themselves. In general, root biomechanics have been difficult to quantify due to the heterogeneous structure and irregular geometry of these organs (Goodman and Ennos, 1998, 2001). Previous studies in maize have aimed to simplify root biomechanics by assuming roots are a solid cylinder and testing only the tip of the root prior to lateral branching (Goodman and Ennos, 1998, 2001). In these studies, a 3-point bend loading approach was used to assess root biomechanics of subterranean lateral and nodal roots of maize (Goodman and Ennos, 1998, 2001). However, in the context of brace roots, the aerial portion of the root that is closest to the stalk is most important for stalk stability, and a comprehensive analysis of spatiotemporal brace root biomechanics has not been performed.

In the context of lodging-resistance, it is important to select mechanical loading configurations that mimic natural failure patterns during root lodging. Root lodging-resistance is a function of the resistance of the compressed leeward roots to bending, and the anchorage of roots under tension

(Coutts, 1986). Although poorly reported in the scientific literature, we have observed that breakage in bending is a common failure mode for maize brace roots during root lodging (Fig. 1A). Therefore, we propose that a 3-point bend loading configuration is most likely to mimic the natural failure patterns of brace roots.

In this study, 3-point bending was used to measure the differences in brace root biomechanics within and between three maize inbred genotypes and across vegetative and reproductive growth stages. The data show that there are differences in brace root structural mechanical properties between whorls that are largely due to brace root geometry. These differences occur regardless of genotype or growth stage. However, a comparison between genotypes shows that bending moduli (E) can be used to differentiate genotypes within a growth stage. These results support the hypothesis that mechanical properties of brace roots contribute to their function in plant mechanical stability.

MATERIALS AND METHODS

Vegetative sample collection (greenhouse)

Seeds from an inbred maize genotype (*Zea mays* cv. B73) were germinated in 3-gallon pots with BK 55 soil (PRO-MIX) and 30 grams of slow release osmocote pellets (Scotts Miracle-Gro). Target greenhouse conditions were 24.7°C day/21.6°C night, 49% day/52% night humidity, and 14 h daylight. Supplemental lighting of 400 Watt High Pressure Sodium and Metal Halide bulbs were used when natural light levels fell below 600 W/m2 (watts per square meter). Plants were watered twice a week until complete soil saturation: (1) with tap water and (2) with tap water mixed with supplemental nutrient solution (Peters Excel 21-5-20 N-P-K). Five biological replicates were grown to the vegetative leaf 13 (V13), V14, and V15 stage based on the “droopy” leaf method (Nielson, 2019). At each growth stage, stalks were cut approximately 15 cm above the TWR and 15 cm beneath the BWR. Brace roots were excised from each whorl and dried in a drying oven at 57°C for a minimum of 24 hours.

Reproductive sample collection (field)

Seeds from three inbred maize genotypes (*Zea mays* cv. B73, *Zea mays* cv. Oh43, and *Zea mays* cv. A632) were planted in two replicate plots in Newark, DE during the summers of 2019 and 2020. In 2020, four brace roots from the top whorl (TWR), middle whorl (MWR), and bottom whorl (BWR) (Fig. 1B) were removed from six plants per genotype at the reproductive stage (R1/2, ~67 days after planting). Roots were placed on a damp paper towel to maintain moisture and subjected

to 3-point bend tests on the same day. In 2019, four brace roots from the MWR and four brace roots from the BWR (Fig. 1B) were removed from six to seven plants per genotype at reproductive maturity (R6, ~123 days after planting) and stored in brown paper bags in a dry field shed for a minimum of 3 months.

Measuring brace root geometry

Brace roots were trimmed to include the first 20 mm closest to the stem (Fig. 1B). Brace root sample diameters were measured with a digital caliper (DC) (NEIKO 01407A, 0-6 inch). Major diameter (majorDC) and minor diameter (minorDC) measurements (Fig. 1C) were taken at the midpoint of the brace root section, which is the loading site during 3-point bending (Fig. 1D).

Micro-computed tomography (microCT) scanning was used as a second estimate of brace root geometry on V13-15 dried roots and R6 roots. Brace root samples were inserted into a low-density upholstery foam fixture to provide a supportive bed that would not appear on the microCT scan and samples were scanned with a Bruker Skyscan 1276 (Settings: pixel size = 42.32 µm, voltage = 40 kV, current = 100 µA, exposure = 203 ms, angular step = 0.4 degrees). Scans were reconstructed using Bruker Nrecon software (Supplementary Fig. S1). Fiji software (Schindelin *et al.*, 2012) was used to measure the following brace root dimensions from the central cross section of microCT scans: distance from the center point to the (1) exterior of the minor outer wall (ao), (2) interior of the minor outer wall wall (ai), (3) interior of the minor inner wall (ai), (4) exterior of the major outer wall (bo), interior of the major outer wall (bi), interior of the major inner wall (bi) (Supplementary Fig. S1G). For V13-15 and R6 roots, major (majorCT) and minor (minorCT) diameters, and major and minor wall thicknesses were calculated using measurements extracted from CT scans. For R1/R2 roots, a digital caliper was used to measure diameters (majorDC and minorDC) in lieu of microCT scanning.

Moment of inertia calculations

Moments of inertia (MOI) were calculated using the following equations, with the consideration that the brace roots can be considered solid elliptical cylinders (Eq. 1) or hollow elliptical cylinders (Eq. 2):

$$MOI_{solid} = \frac{\pi}{4}\,(a_o^3 b_o) \qquad \text{(Eq. 1)}$$

$$MOI_{hollow} = \frac{\pi}{4}\left(a_o^3 b_o - a_i^3 b_i\right) \qquad \text{(Eq. 2)}$$

where π = 3.1415, a_o is the minor outer radius (distance from the center to the short side exterior wall of the cortex), b_o is the major outer radius (distance from the center to the long side exterior wall of the cortex), a_i is the minor inner radius (distance from the center to the short side interior wall of the cortex), and b_i is the major inner radius (distance from the center to the long side interior wall of the cortex) (Supplementary Fig. S1G). For all comparative calculations, the equation for solid cylinder MOI was used.

True MOI was measured from the microCT scanned images. Each sample was aligned in three dimensions in DataViewer (Bruker, Belgium) to get aligned cross sectional stacks. Images were thresholded to separate the roots from the background. MOI was then calculated using a 2D analysis function for each thresholded sample at the mid-length, using CT Analyzer software (Bruker, Belgium).

3-point bend testing

A custom 3-point bend fixture was machined with a 17 mm span length (Fig. 1D). Samples were tested using an Instron 5943 (Norwood, Massachusetts USA) equipped with a 100 N load cell (Instron 2530 Series static load cell, Norwood, Massachusetts USA). Each brace root sample was placed on the fixture and adjusted for midpoint loading, in which the top fixture was moved to come in contact with the sample at its mid-length. Prior to testing, each sample was preloaded to 0.2 N and the displacement readout was calibrated. Samples were loaded in compression at a constant rate of 1 mm/min until failure. Force-displacement data were captured with Bluehill 3 software (Instron, Norwood, Massachusetts USA). Testing continued until failure, which was defined as the first steep decline in the force-displacement curve and characterized as a crack forming in the brace root sample opposite of the loading site. Structural stiffness (K) was defined as the linear slope of the force-displacement curve (Fig. 2A). Ultimate Load (UL) was defined as the highest force the sample withstood without failure (Fig. 2A). Break Load (BL) was defined as the force upon fracture, illustrated as the first sharp drop in the force-displacement curve (Fig. 2A). All K were extracted from force-displacement curves using Bluehill 3 software. UL and BL were extracted using a custom Python code. To normalize structural stiffness measurements for geometry, K was converted to bending modulus (*E*), using the equation for a center loaded beam fixed at both ends (Eq. 3):

$$E = K\,x\,\frac{L^3}{48MOI} \qquad \text{(Eq. 3)}$$

where *E* is the bending modulus, *K* is the structural stiffness, *L* is the fixture span length, and *MOI* is the moment of inertia for the solid cylinder assumption (Eq. 3 adapted from Al-Zube *et al.*, 2018).

Quality Control

Data were quality controlled for both the microCT scan (CT) and the 3-point bend tests (M). Brace root microCT scans were scored independently by two scientists according to the following criteria: CT1: Shaped like a figure 8, CT2: Irregularly shaped, CT3: Inner wall biased towards one side, CT4: A combination of CT1-CT3, or None (Supplementary Fig. S1C-F). 3-point bend tests were classified as follows: M1: sample too short, curved, or splintered during testing, M2: break load occurred before ultimate load, or None. Samples scored as M2 or None were retained for analysis (Supplementary Fig. S1B).

Data analysis

We used a one-way analysis of variance (ANOVA) to determine if there were statistical differences between whorls of B73 plants within each growth stage for brace root structural mechanical properties, brace root geometry, and brace root material properties. For V13-15 samples, brace root whorls were nested within vegetative stage. For R1/R2 and R6 samples, whorls were compared among biological replicates. To determine if the variation in brace root mechanical and material properties between whorls was conserved in other taxa, two additional genotypes were tested at the R1/R2 and R6 growth stage (as described above). Within each maize genotype, an ANOVA was used to determine if there were statistical differences between the R1/2 and R6 growth stage for brace root structural mechanical and material properties. Further, the brace root structural mechanical and material properties of A632 and Oh43 were normalized by B73 and compared within each whorl. All data analysis was performed in R (version 4.0.3) statistical computing software with default parameters (R Core Team, 2013). All figures were generated in R with the ggplot2 (version 3.3.1) data visualization package (Wickham, 2016).

RESULTS

Brace root structural mechanical properties vary between whorls, which can be attributed to differences in geometry.

We hypothesized that brace root mechanical properties vary between whorls, and thus may contribute to the differential contribution of brace roots to stalk anchorage (Reneau *et al.*, 2020). To test this hypothesis, 3-point bend tests were applied to brace roots from two-to-three whorls from one maize genotype (B73) at different vegetative and reproductive growth stages: V13-15, R1/2, and R6. A comparison of 3-point bend results shows that the structural stiffness (K) and ultimate load (UL) are significantly decreased from BWR to TWR for all three growth stages (Fig. 2B-D; Supplementary Table S1). The break load (BL) was significantly decreased from BWR to TWR for R1/R2 and R6 field samples, but no statistical difference in BL between whorls was observed in V13-15 greenhouse samples (Figure 2B-D, Supplementary Table S1). These results show that brace roots from whorls closest to the soil have higher structural mechanical properties than brace roots from whorls further from the soil, and differences between whorls become more distinct in older plants.

The differences in structural mechanical properties can be due to differences in geometry and/or the material properties of brace root samples. Here, the geometry of B73 brace roots was measured at the site of loading (approximately 10 mm from the brace root base) by microCT and/or a digital caliper. There was a high positive correlation for diameter measurements between both approaches (minor diameter r = 0.87, major diameter r = 0.87; Supplementary Fig. S2). In all three growth stages, the major and minor brace root diameters (Fig. 3A) decrease from BWR to TWR (Fig. 3B-C). The major and minor wall thickness were also significantly different between whorls, with the TWR having thinner wall thickness than the BWR (Supplementary Fig. S3). These results demonstrate that both diameter and wall thickness may influence the structural mechanical properties of brace roots.

To determine if the structural mechanical properties within a genotype are influenced by material properties, the bending modulus (E) was calculated based on a solid cylinder assumption. In R1/2 and R6 field samples, B73 brace roots did not differ in material properties between whorls (Fig. 4). However, in dried V13-15 greenhouse samples, the brace roots from the TWR had a greater E compared to brace roots from either the MWR or BWR (Fig. 4). These results are likely attributed to the age of roots at the time of sampling. At V13-15, the TWR brace roots are the

236 “youngest”, having recently emerged from the stem. Thus, the developmental age of the roots
237 themselves may also influence the bending modulus.
238
239 Differences in brace root structural mechanical properties between whorls are observed in two
240 additional maize genotypes
241 To determine if whorl-specific brace root biomechanics are unique to B73 or common across other
242 genotypes, R1/2 and R6 field samples from two additional genotypes (*Zea mays* cvs. A632 and
243 Oh43) were subject to 3-point bending. Similar to B73, structural mechanical properties (K, UL,
244 and BL) decrease from TWR to BWR in both reproductive growth stages (Fig. 5; Supplementary
245 Table S1). Further, brace root diameters also varied for A632 and Oh43 in both reproductive
246 growth stages, with brace roots from the highest whorls having smaller diameters
247 (Supplementary Fig. S5). Therefore, when accounting for the geometry of A632 and Oh43 by
248 calculating E, the majority of within plant variation was reduced (Fig. 5). One exception is the
249 A632 brace root samples from R1/R2 conditions. These roots have a significantly different E
250 between the TWR and the MWR, with the TWR having a larger E than the BWR (Fig. 5D).
251
252 Plant growth stage affects brace root mechanical properties.
253 The impact of root lodging increases with plant maturity (Carter and Hudelson, 1988), and thus
254 we wanted to understand the variation in brace root biomechanics between R1/2 and R6 growth
255 stages. Brace root biomechanical data was compared between the two stages within a whorl and
256 genotype (Fig. 6; Supplementary Table S2). For all comparison, the UL was significantly higher
257 for R1/2 brace roots compared to R6 brace roots (Fig. 6A). The same was true for the BL, except
258 for Oh43 BWR brace roots (Fig. 6B). These results demonstrate that the force needed to cause
259 failure (UL and BL) decreases during reproductive maturity, which may affect the frequency and
260 impact of lodging.
261
262 In contrast to UL and BL, the relationship between R1/R2 and R6 samples for K and E was
263 variable by both genotype and whorl (Fig. 6C-D). Specifically, B73 had a higher K at R1/2 for both
264 whorls. Whereas, A632 had a higher K at R1/2 for MWR brace roots only, and Oh43 showed no
265 differences in K between growth stages for either whorl. These differences were retained upon
266 calculation of E (Fig. 6D), and thus cannot be solely attributed to differences in geometry. Instead,
267 these results indicate that the variation in brace root stiffness and bending modulus throughout
268 reproductive maturity is genotype- and whorl-dependent. This is likely a result of differences in

material properties and/or the variable within-genotype dynamics of plant senescence (i.e. rate of water loss).

The relationship between genotypes is constant for material properties, but not structural mechanical properties.

Given the variation between genotypes and whorls, we aimed to understand the relative relationship of brace root biomechanics between genotypes at a given growth stage and whorl. Least square means were calculated for the mechanical properties of brace roots from A632 and Oh43 and normalized by those of B73. The relative relationship between genotypes is variable for structural mechanical properties both within and between whorls, and between growth stages (Fig. 7). For all whorls and conditions, the E for A632 is relatively higher, whereas the E for B73 and Oh43 are closely related (Fig. 7). These results demonstrate that there are differences in brace root material property that can be used to differentiate between genotypes at a similar growth stage.

Brace root bending moduli are similar to the bending moduli of other maize tissues at similar stages.

The E for R1/2 and R6 brace roots were compared with previous studies (Fig. 8; Supplementary Table S3). These previous data include measurements of 1) senesced maize stalks (Al-Zube *et al.*, 2018), 2) maize nodal roots grown hydroponically (Goodman and Ennos, 2001), 3) fresh maize stems (Goodman and Ennos, 1996), and 4) first order maize lateral roots (Goodman and Ennos, 1998). For studies 2-4, maize organs were assumed to have a solid cylinder geometry and measured with 3-point bend tests. However, for study 1, the bending modulus was calculated for the rind tissue only (Al-Zube *et al.*, 2018) since previous results demonstrated that the contribution of stalk pith was negligible (Al-Zube *et al.*, 2017). This meta-analysis shows that E for R6 brace roots is comparable to senesced stems, and E for R1/2 brace roots is comparable to fresh stems and roots (Fig. 8).

DISCUSSION

In this study, we identified differences in the mechanical properties for brace roots originating from different whorls. Specifically, brace roots closer to the ground had increased stiffness and load-carrying capacity compared to brace roots from higher whorls. These results are consistent with the brace roots closer to the soil contributing the most to stalk anchorage and therefore needing

302 increased resistance to bending and breakage. We also measured differences in geometry of
303 brace roots from different whorls that reflected the differences in mechanical properties.
304 Differences between whorls within a genotype are primarily attributed to these changes in
305 geometry, whereas differences between genotypes can be attributed to differences in the
306 underlying material properties. Overall, these results support the hypothesis that variable brace
307 root mechanical properties between whorls may contribute to the differential contribution of brace
308 roots to stalk anchorage.

309 The geometry of brace roots was assumed to be a solid elliptical solid cylinder based on previous
310 reports (Goodman and Ennos, 1998, 2001). However, microCT scans of brace roots revealed
311 that the roots may alternatively be considered as a hollow tube (Supplementary Fig. S1). To test
312 the validity of the solid cylinder assumption, E and MOI for V13-15 brace roots calculated using
313 the solid cylinder and hollow cylinder assumptions (Supplementary Fig. S5A-B). The regression
314 of these data indicate that solid and hollow assumptions are highly positively correlated (MOI:
315 r=0.99, E: r=0.99). Since the void space within brace root samples is small, the difference between
316 solid and hollow MOI and E calculations was negligible. To test the validity of the cylindrical
317 geometric assumption, the true MOI was calculated for a subset of R6 B73 brace roots using
318 microCT scans (Supplementary Fig. S5C). A regression between the solid cylinder MOI and true
319 MOI shows a high positive correlation (r=0.79), which indicates that the MOI assumptions are
320 reasonable approximations for brace root geometry.
321
322 Our results show that differences in brace root biomechanics within a genotype are due to
323 geometry, whereas differences between genotypes can be attributed to both geometry and
324 material properties. These results were constant within vegetative and reproductive growth
325 stages. The biology underlying the variation in biomechanics between genotypes is an area for
326 future investigation. Differences in cell wall composition or arrangement, the number of vascular
327 cylinders and vascular area (Yu *et al.*, 2015), and/or the dynamics of senescence (i.e. rate of
328 water loss) are likely candidates as the source(s) of variation. Understanding this biological
329 variation is the key to improving the brace root contribution to anchorage. The results presented
330 here provide the foundation for widespread evaluation of brace root mechanical properties and
331 understanding their link to plant mechanical stability.
332

SUPPLEMENTARY DATA

Figure S1. Quality control and geometry measurements of maize brace root microCT scans.

Figure S2. MicroCT and caliper geometry measurements are highly positively correlated.

Figure S3. Brace root wall thickness is significantly different between whorls.

Figure S4. Brace root diameters differ between whorls for A632 and Oh43.

Figure S5. The solid and hollow cylinder assumptions are highly correlated.

Table S1: Summary of ANOVA comparisons within genotype and growth stage.

Table S2: Summary of ANOVA comparison between reproductive stages.

Table S3: Bending moduli of maize organs.

ACKNOWLEDGEMENTS

We gratefully acknowledge the members of the Sparks lab for assistance in harvesting plants, collecting brace roots, and preparing brace root samples. We additionally acknowledge Richard West and The Center for Biomedical and Brain Imaging (CBBI) for microCT assistance, Dr. Dawn Elliott (University of Delaware) for access to Instron, Dr. Douglas Cook (Brigham Young University) for assistance identifying foam support for microCT scanning, and Dr. Rubén Rellán-Álvarez (University of North Carolina) for providing the picture of root lodging. This research was made possible by funding from the University of Delaware Research Foundation and the Thomas Jefferson Fund to EES.

AUTHOR CONTRIBUTIONS

Conceptualization: EES and MLK

Formal analysis: LE, EG, and ANH

Funding acquisition: EES

Investigation: LE

Methodology: LE, EG, ANH, MLK and EES

Software: AS

Supervision: EES and MLK

Visualization: LE

Writing - original draft: LE and EES

Writing - review & editing: LE, EG, ANH, MLK, and EES

DATA AVAILABILITY STATEMENT

All raw data and R scripts used to process and analyze data are available at: https://github.com/EESparksLab/Erndwein_et_al_2021.

REFERENCES

Al-Zube LA, Robertson DJ, Edwards JN, Sun W, Cook DD. 2017. Measuring the compressive modulus of elasticity of pith-filled plant stems. Plant methods **13**, 99.

Al-Zube L, Sun W, Robertson D, Cook D. 2018. The elastic modulus for maize stems. Plant methods **14**, 11.

Berry PM, Sterling M, Spink JH, Baker CJ, Sylvester-Bradley R, Mooney SJ, Tams AR, Ennos AR. 2004. Understanding and reducing lodging in cereals. Advances in Agronomy **84**, 215–269.

Blizard S, Sparks EE. 2020. Maize Nodal Roots. Annual Plant Reviews online, 281–304.

Carter PR, Hudelson KD. 1988. Influence of simulated wind lodging on corn growth and grain yield. Journal of Production Agriculture **1**, 295–299.

Coutts MP. 1986. Components of Tree Stability in Sitka Spruce on Peaty Gley Soil. Forestry **59**, 173–197.

Fedenko JR, Erickson JE, Singh MP. 2015. Root lodging affects biomass yield and carbohydrate composition in sweet sorghum. Industrial crops and products **74**, 933–938.

Feldman L. 1994. The Maize Root. The Maize Handbook, 29–37.

Flint-Garcia SA, Jampatong C, Darrah LL, McMullen MD. 2003. Quantitative Trait Locus Analysis of Stalk Strength in Four Maize Populations. Crop Science **43**, 13.

Forell GV, Robertson D, Lee SY, Cook DD. 2015. Preventing lodging in bioenergy crops: a biomechanical analysis of maize stalks suggests a new approach. Journal of experimental botany **66**, 4367–4371.

Goodman AM, Ennos AR. 1996. A comparative study of the response of the roots and shoots of sunflower and maize to mechanical stimulation. Journal of experimental botany **47**, 1499–1507.

Goodman AM, Ennos AR. 1998. Responses of the Root Systems of Sunflower and Maize to Unidirectional Stem Flexure. Annals of botany **82**, 347–357.

Goodman AM, Ennos AR. 2001. The Effects of Mechanical Stimulation on the Morphology and Mechanics of Maize Roots Grown in an Aerated Nutrient Solution. International journal of plant sciences **162**, 691–696.

Hochholdinger F. 2009. The Maize Root System: Morphology, Anatomy, and Genetics. In: Bennetzen JL,, In: Hake SC, eds. Handbook of Maize: Its Biology. New York, NY: Springer New York, 145–160.

Hochholdinger F, Woll K, Sauer M, Dembinsky D. 2004. Genetic Dissection of Root Formation in Maize (Zea mays) Reveals Root-type Specific Developmental Programmes. Annals of botany **93**, 359–368.

Hoppe DC, McCully ME, Wenzel CL. 1986. The nodal roots of Zea: their development in relation

to structural features of the stem. Canadian journal of botany. Journal canadien de botanique **64**, 2524–2537.

Hostetler AN, Khangura RS, Dilkes BP, Sparks EE. 2020. Bracing for sustainable agriculture: the development and function of brace roots in members of Poaceae. Accepted at Current Opinion in Plant Biology.

Liu S, Song F, Liu F, Zhu X, Xu H. 2012. Effect of Planting Density on Root Lodging Resistance and Its Relationship to Nodal Root Growth Characteristics in Maize (Zea mays L.). Journal of Agricultural Science **4**, 182.

Nielson RL. 2019. Determining corn leaf stages. Kingcorn.org.

R Core Team. 2013. R: A language and environment for statistical computing.

Rajkumara S. 2008. Lodging in cereals-a review. Agricultural reviews **29**, 55–60.

Reneau JW, Khangura RS, Stager A, Erndwein L, Weldekidan T, Cook DD, Dilkes BP, Sparks EE. 2020. Maize brace roots provide stalk anchorage. Plant Direct, 2020.07.28.225656.

Schindelin J, Arganda-Carreras I, Frise E, *et al.* 2012. Fiji: an open-source platform for biological-image analysis. Nature methods **9**, 676–682.

Sekhon RS, Joyner CN, Ackerman AJ, McMahan CS, Cook DD, Robertson DJ. 2020. Stalk Bending Strength is Strongly Associated with Maize Stalk Lodging Incidence Across Multiple Environments. Field crops research **249**, 107737.

Sharma S, Carena MJ. 2016. BRACE: A Method for High Throughput Maize Phenotyping of Root Traits for Short-Season Drought Tolerance. Crop science **56**, 2996–3004.

Shi J, Drummond BJ, Habben JE, *et al.* 2019. Ectopic expression of ARGOS8 reveals a role for ethylene in root-lodging resistance in maize. The Plant Journal **97**, 378–390.

Stubbs CJ, Seegmiller K, McMahan C, Sekhon RS, Robertson DJ. 2020. Diverse maize hybrids are structurally inefficient at resisting wind induced bending forces that cause stalk lodging. Plant Methods **16**.

Tirado SB, Hirsch CN, Springer NM. 2020. Utilizing Temporal Measurements from UAVs to Assess Root Lodging in Maize and its Impact on Productivity. , 2020.05.21.108746.

Wickham H. 2016. ggplot2: Elegant Graphics for Data Analysis. Springer.

Yu P, Hochholdinger F, Li C. 2015. Root-type-specific plasticity in response to localized high nitrate supply in maize (Zea mays). Annals of botany **116**, 751–762.

FIGURE LEGENDS

Figure 1. Methods for measuring biomechanics of maize brace roots.

A) Breakage through bending is a common failure mode for brace roots during lodging. B) In this study, BWR (bottom whorl) indicates roots emerging from nodes closest to the soil, MWR (middle whorl) indicates roots from the next node shootward, and TWR (top whorl) indicates the node furthest away from the soil. The first 20 mm of each brace root was used for testing. C) The moment of inertia (MOI) was calculated with the assumption that brace roots are solid elliptical cylinders. The major (b_o) and minor (a_o) diameters were measured from microCT scans and digital calipers. D) The 3-point bend fixture was 17 mm with the load cell anvil applied to the center of the brace root sample at a constant rate of displacement until fracture.

Figure 2. Structural mechanical properties differ between brace root whorls.

A) Structural mechanical properties are extracted from the 3-point bending force-displacement curve. These properties include: structural stiffness (K), ultimate load (UL), break load (BL). K, UL, and BL decrease from BWR to TWR for all three growth stages: B) V13-15, C) R1/2, D) R6. TWR = top whorl, MWR = middle whorl; BWR = bottom whorl. Gray bars indicate Tukey HSD $p<0.01$.

Figure 3. The diameter of maize brace roots varies between whorls.

A) Brace root major diameter and minor diameter were measured for all growth stages. For all growth stages, the TWR has a lower major (B) and minor (C) diameter than MWR and BWR. TWR = top whorl, MWR = middle whorl; BWR = bottom whorl. Gray bars indicate Tukey HSD $p<0.01$.

Figure 4. The material properties of brace roots are constant during reproductive, but not vegetative growth stages.

The bending modulus (E) of B73 brace root samples from three growth stages was calculated under a solid cylinder assumption. For R1/2 and R6 field stages, E of maize brace roots does not vary significantly between whorls. For V13-15 greenhouse stages, E of TWR brace roots is significantly different from E of MWR and BWR brace roots. TWR = top whorl, MWR = middle whorl; BWR = bottom whorl. Gray bars indicate Tukey HSD $p<0.01$.

Figure 5. Within genotype variation in brace root biomechanics is consistent for two additional genotypes.

To determine if B73 biomechanical observations can be extended to other maize genotypes, brace roots from A632 and Oh43 at R1/2 and R6 were 3-point bend tested. As with B73, A) UL, B) BL, and C) K decrease from BWR to TWR. D) Calculating bending modulus (E) again reduces the differences between whorls. TWR = top whorl, MWR = middle whorl; BWR = bottom whorl. Gray bars indicate Tukey HSD $p<0.01$.

Figure 6. Growth stage affects brace root biomechanics in a genotype- and whorl-specific manner.

Mechanical properties were compared between R1/2 and R6 conditions within a whorl and within a genotype. A) UL was higher in all genotypes and all whorls at R1/2 as compared to R6. B) BL was higher in all genotypes and all whorls R1/2, with the exception of Oh43 BWR brace roots, which did not reach the significance threshold. C) A632 brace roots had a higher K at R1/2 only for the MWR; B73 brace roots had a higher K at R1/2 for both BWR and MWR; Oh43 brace roots were not significantly different for K between growth stages for either whorl. D) A632 brace roots had a lower E at R1/2 only for the MWR; B73 brace roots had a lower E at R1/2 for both BWR and MWR; Oh43 brace roots were not significantly different for E between growth stages for either whorl. MWR = middle whorl; BWR = bottom whorl. Gray bars indicate Tukey HSD $p<0.01$.

Figure 7. The normalized order of genotypes is consistent for bending modulus, but not structural mechanical properties.

Least square means were calculated for the mechanical properties of brace roots from inbred maize genotypes A632 and Oh43 and normalized by those of B73. For K, UL, and BL, the order of genotypes varied within and between whorls, and between growth stages. In contrast, the order of genotypes was more consistent between all whorls and growth stages when utilizing E as the comparative metric.

Figure 8. Bending moduli of maize brace roots is comparable to other maize organs.

Among all growth stages and genotypes, the majority of maize brace roots measured in this study had bending moduli between 0.14 and 23 GPa. This E range is comparable with that of other maize organs that have been reported in the literature (see also Supplementary Table S3).

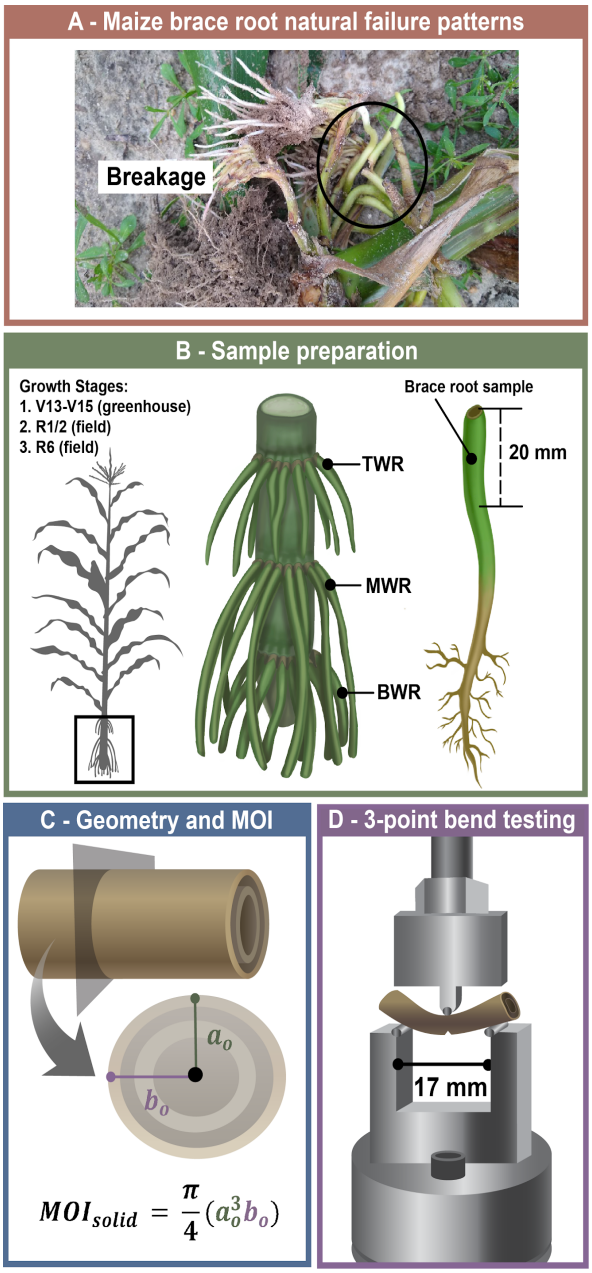

Figure 1. Methods for measuring biomechanics of maize brace roots.

A) Breakage through bending is a common failure mode for brace roots during lodging. B) In this study, BWR (bottom whorl) indicates roots emerging from nodes closest to the soil, MWR (middle whorl) indicates roots from the next node shootward, and TWR (top whorl) indicates the node furthest away from the soil. The first 20 mm of each brace root was used for testing. C) The moment of inertia (MOI) was calculated with the assumption that brace roots are solid elliptical cylinders. The major (b_o) and minor (a_o) diameters were measured from microCT scans and digital calipers. D) The 3-point bend fixture was 17 mm with the load cell anvil applied to the center of the brace root sample at a constant rate of displacement until fracture.

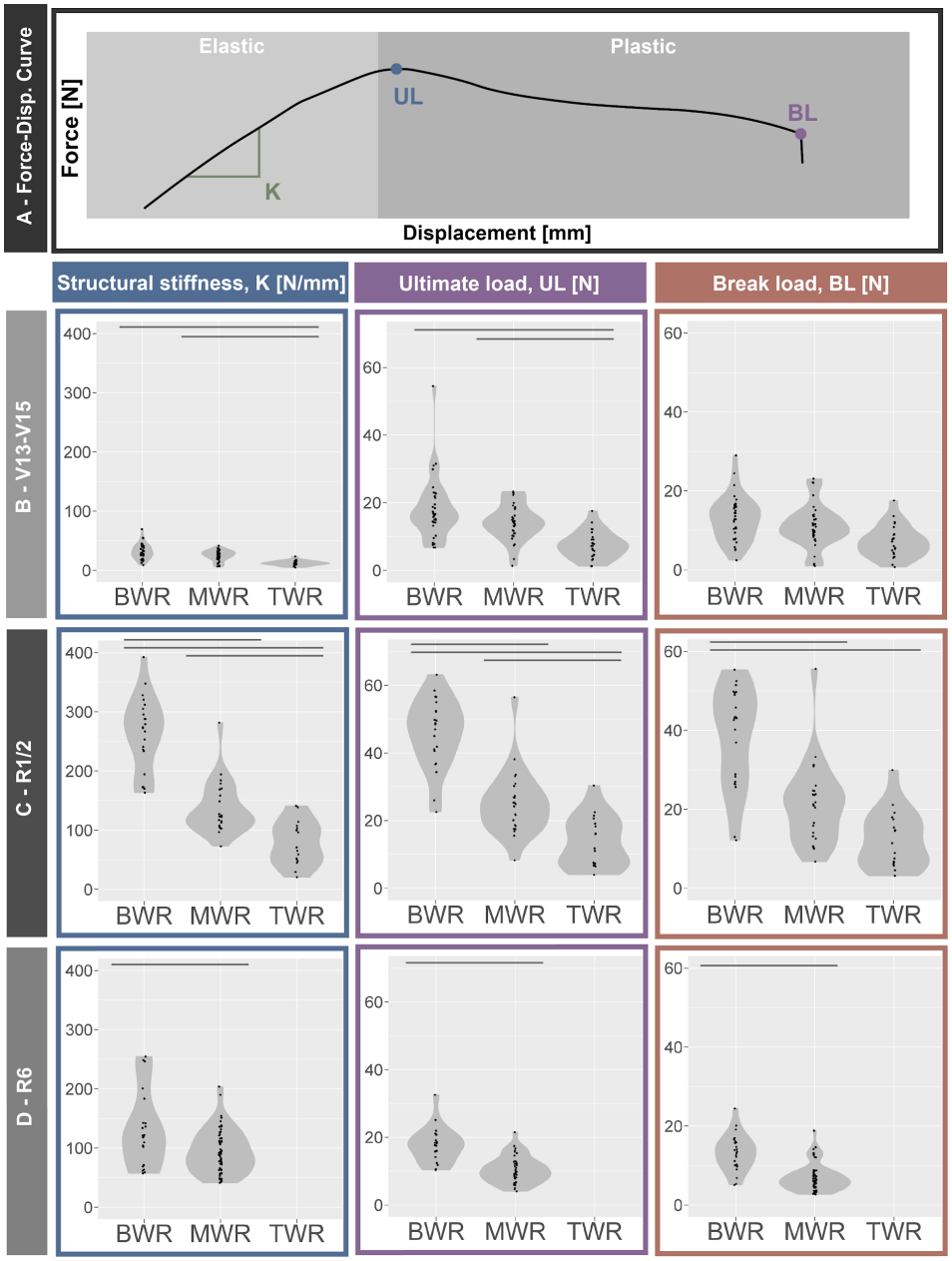

Figure 2. Structural mechanical properties differ between brace root whorls at vegetative and reproductive stages.

A) Structural mechanical properties are extracted from the 3-point bending force-displacement curve. These properties include: structural stiffness (K), ultimate load (UL), break load (BL). K, UL, and BL decrease from BWR to TWR for all three growth stages: B) V13-15, C) R1/2, D) R6. TWR = top whorl, MWR = middle whorl; BWR = bottom whorl. Gray bars indicate Tukey HSD $p<0.01$.

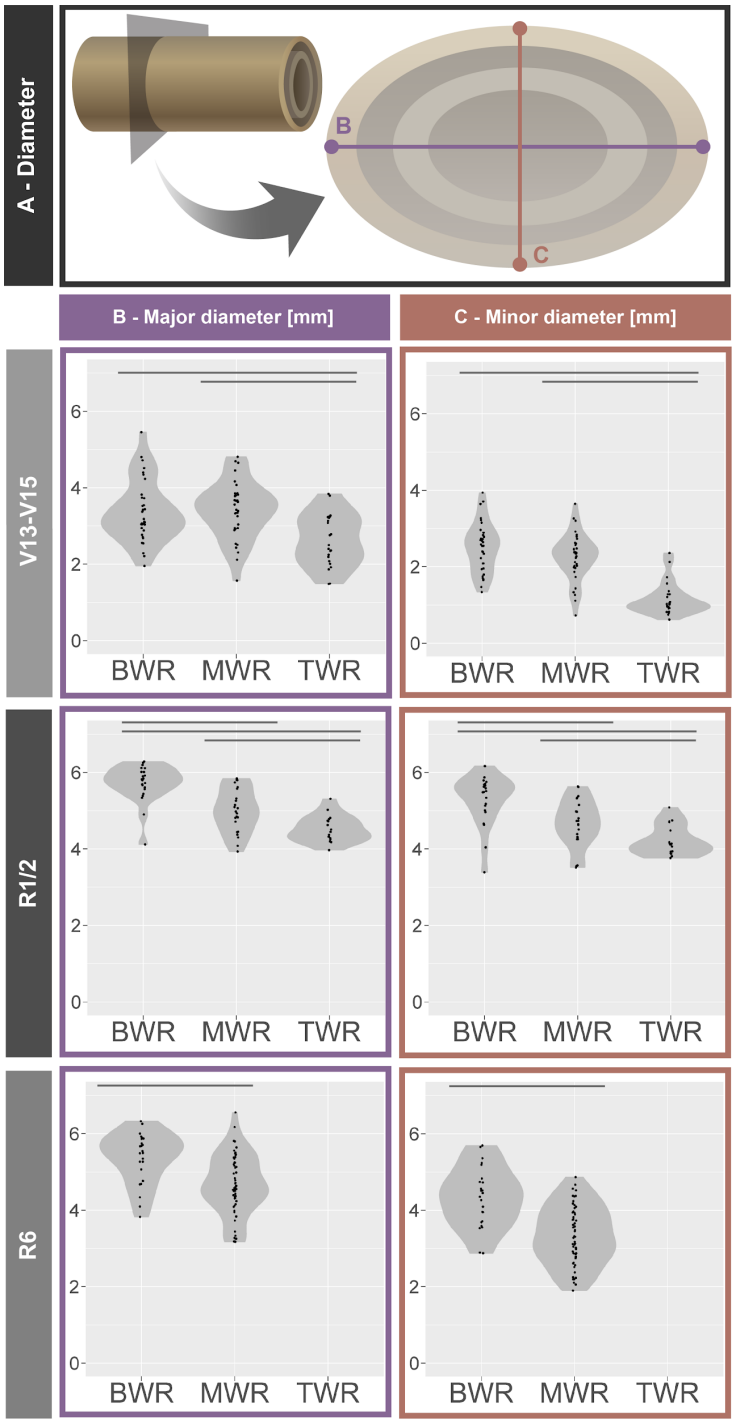

Figure 3. The diameter of maize brace roots varies between whorls.

A) Brace root major diameter and minor diameter were measured for all growth stages. For all growth stages, the TWR has a lower major (B) and minor (C) diameter than MWR and BWR. TWR = top whorl, MWR = middle whorl; BWR = bottom whorl. Gray bars indicate Tukey HSD $p<0.01$.

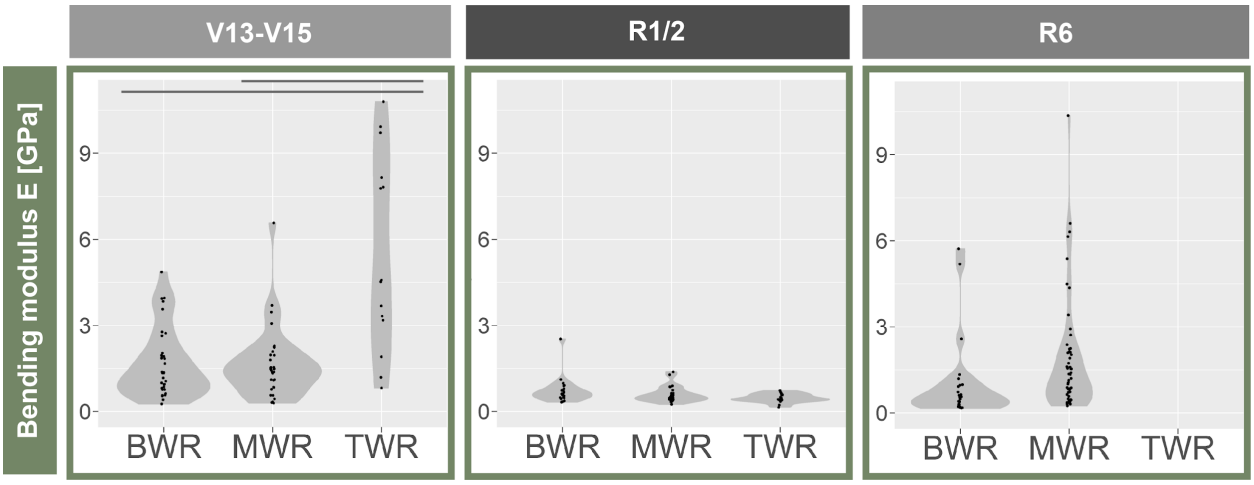

Figure 4. The material properties of brace roots are constant in reproductive, but not vegetative growth stages.

The bending modulus (E) of B73 brace root samples from three growth stages was calculated under a solid cylinder assumption. For R1/2 and R6 field stages, E of maize brace roots does not vary significantly between whorls. For V13-15 greenhouse stages, E of TWR brace roots is significantly different from E of MWR and BWR brace roots. TWR = top whorl, MWR = middle whorl; BWR = bottom whorl. Gray bars indicate Tukey HSD $p<0.01$.

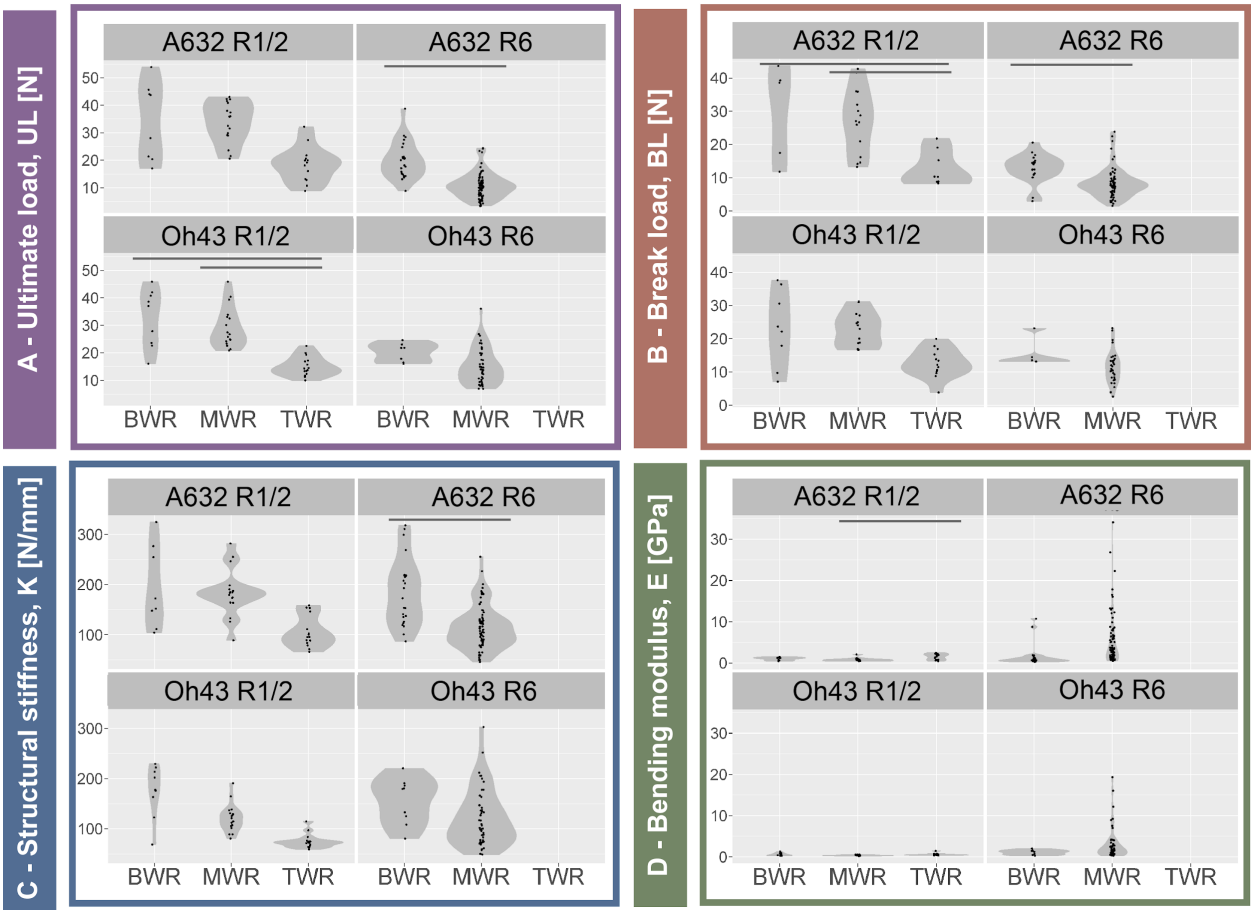

Figure 5. Within genotype variation in brace root biomechanics is consistent for two additional genotypes.

To determine if B73 biomechanical observations can be extended to other maize genotypes, brace roots from A632 and Oh43 at R1/2 and R6 were 3-point bend tested. As with B73, A) UL, B) BL, and C) K decrease from BWR to TWR. D) Calculating bending modulus (E) again reduces the differences between whorls. TWR = top whorl, MWR = middle whorl; BWR = bottom whorl. Gray bars indicate Tukey HSD $p<0.01$.

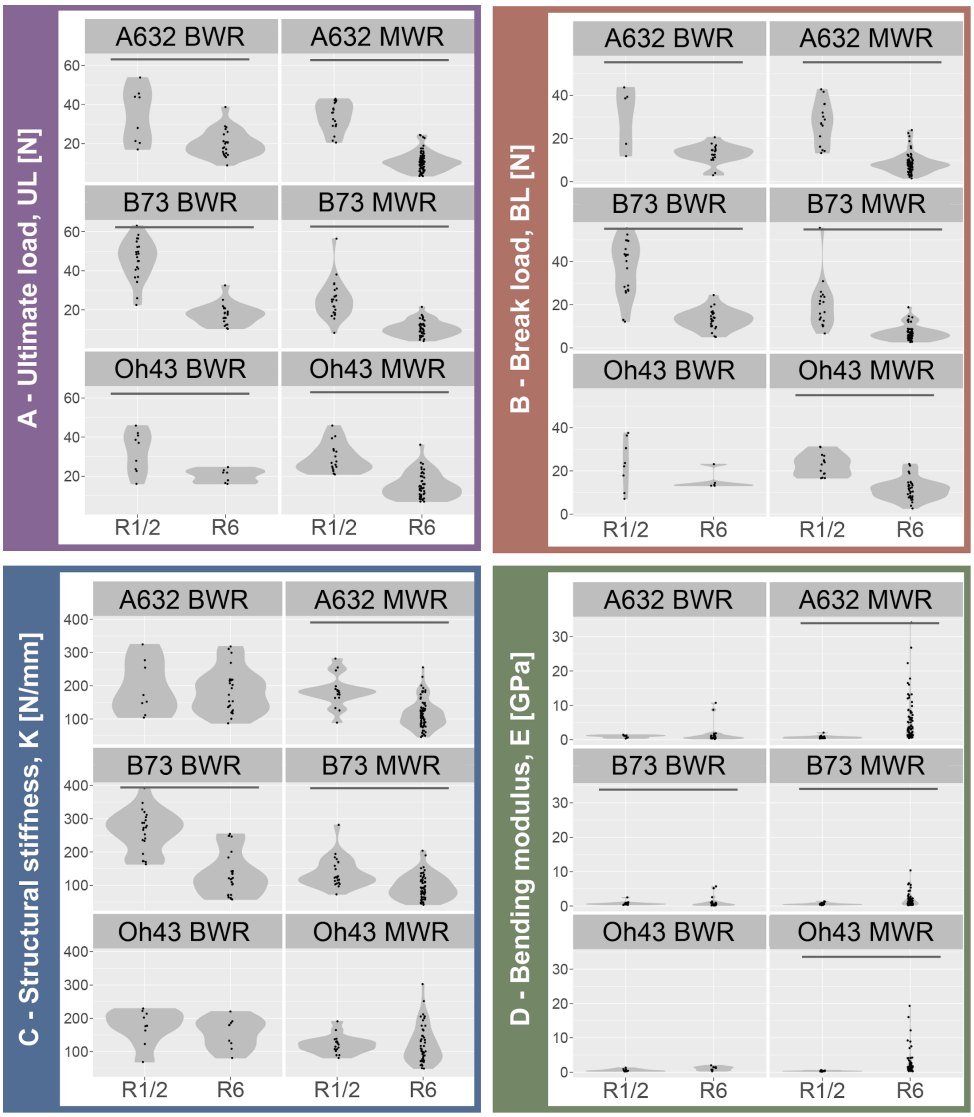

Figure 6. Growth stage affects brace root biomechanics in a genotype- and whorl-specific manner.

Mechanical properties were compared between R1/2 and R6 conditions within a whorl and within a genotype. A) UL was higher in all genotypes and all whorls at R1/2 as compared to R6. B) BL was higher in all genotypes and all whorls R1/2, with the exception of Oh43 BWR brace roots, which did not reach the significance threshold. C) A632 brace roots had a higher K at R1/2 only for the MWR; B73 brace roots had a higher K at R1/2 for both BWR and MWR; Oh43 brace roots were not significantly different for K between growth stages for either whorl. D) A632 brace roots had a lower E at R1/2 only for the MWR; B73 brace roots had a lower E at R1/2 for both BWR and MWR; Oh43 brace roots were not significantly different for E between growth stages for either whorl. MWR = middle whorl; BWR = bottom whorl. Gray bars indicate Tukey HSD $p<0.01$.

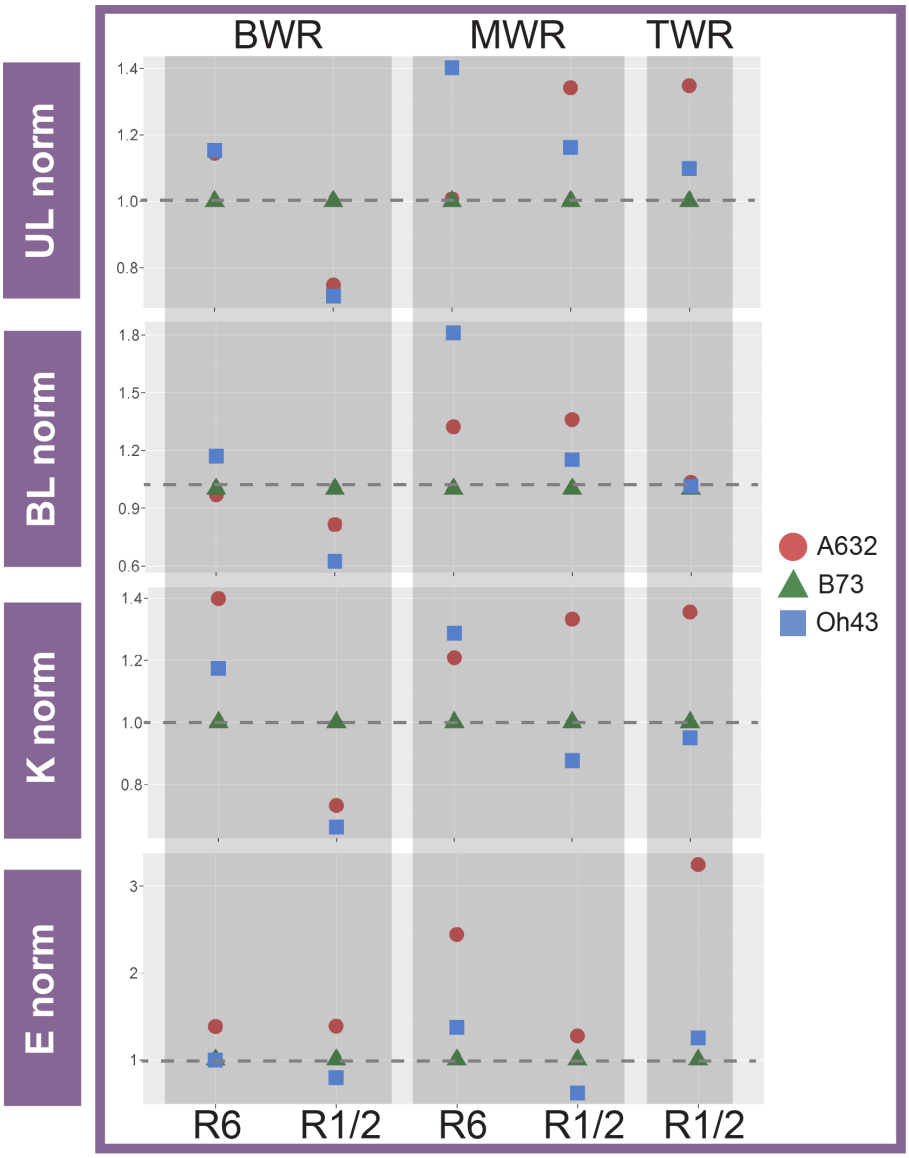

Figure 7. The normalized order of genotypes is consistent for bending modulus, but not structural mechanical properties.

Least square means were calculated for the mechanical properties of brace roots from inbred maize genotypes A632 and Oh43 and normalized (norm) by those of B73. For K, UL, and BL, the order of genotypes varied within and between whorls, and between growth stages. In contrast, the order of genotypes was more consistent between all whorls and growth stages when utilizing E as the comparative metric.

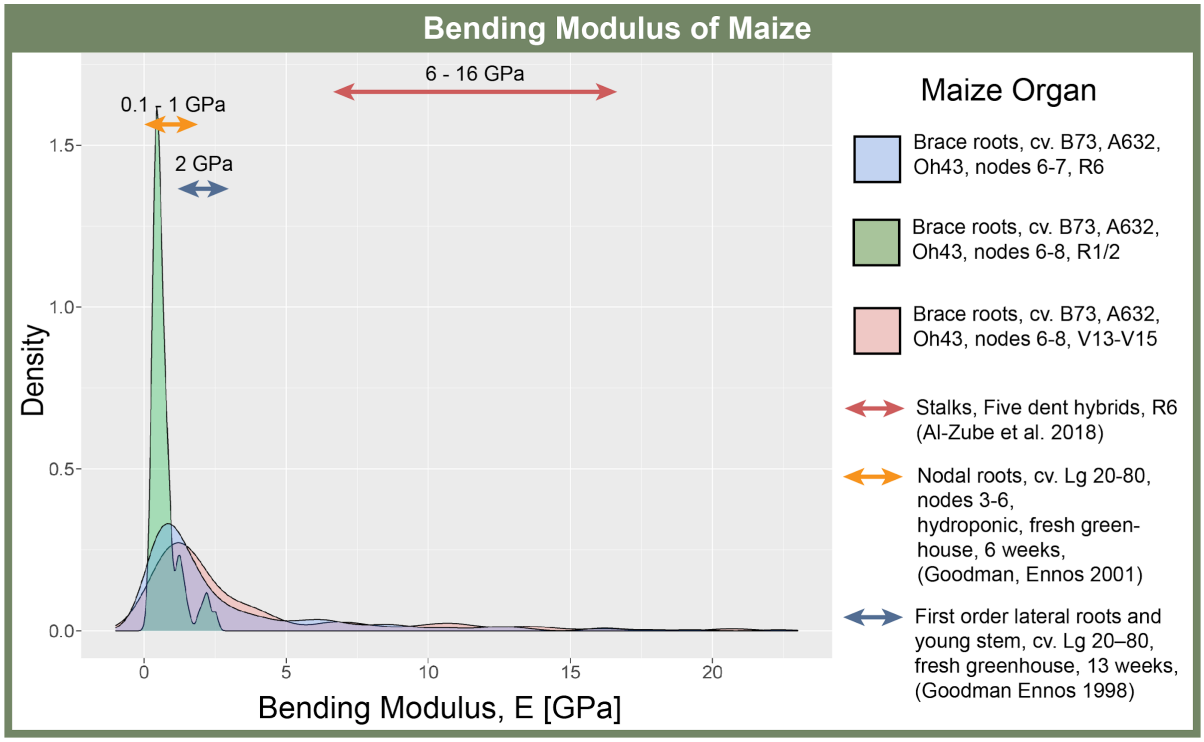

Figure 8. Bending moduli of maize brace roots is comparable with those of other maize organs.

Among all growth stages and genotypes, the majority of maize brace roots measured in this study had bending moduli between 0.14 and 23 GPa. This E range is comparable with that of other maize organs that have been reported in the literature (see also Supplementary Table S3).